CHEMISTRY OF MATERIALS

Subscriber access provided by Binghamton University | Libraries

Article

# Quantum dots in visible light photoredox catalysis: Reductive dehalogenations and C–H arylation reactions using aryl bromides

Anuushka Pal, Indrajit Ghosh, Sameer Sapra, and Burkhard König

*Chem. Mater.*, **Just Accepted Manuscript** • Publication Date (Web): 06 Jun 2017

**Downloaded from http://pubs.acs.org on June 7, 2017**

**Just Accepted**

“Just Accepted” manuscripts have been peer-reviewed and accepted for publication. They are posted online prior to technical editing, formatting for publication and author proofing. The American Chemical Society provides “Just Accepted” as a free service to the research community to expedite the dissemination of scientific material as soon as possible after acceptance. “Just Accepted” manuscripts appear in full in PDF format accompanied by an HTML abstract. “Just Accepted” manuscripts have been fully peer reviewed, but should not be considered the official version of record. They are accessible to all readers and citable by the Digital Object Identifier (DOI®). “Just Accepted” is an optional service offered to authors. Therefore, the “Just Accepted” Web site may not include all articles that will be published in the journal. After a manuscript is technically edited and formatted, it will be removed from the “Just Accepted” Web site and published as an ASAP article. Note that technical editing may introduce minor changes to the manuscript text and/or graphics which could affect content, and all legal disclaimers and ethical guidelines that apply to the journal pertain. ACS cannot be held responsible for errors or consequences arising from the use of information contained in these “Just Accepted” manuscripts.

ACS Publications

Chemistry of Materials is published by the American Chemical Society. 1155 Sixteenth Street N.W., Washington, DC 20036

Published by American Chemical Society. Copyright © American Chemical Society. However, no copyright claim is made to original U.S. Government works, or works produced by employees of any Commonwealth realm Crown government in the course of their duties.

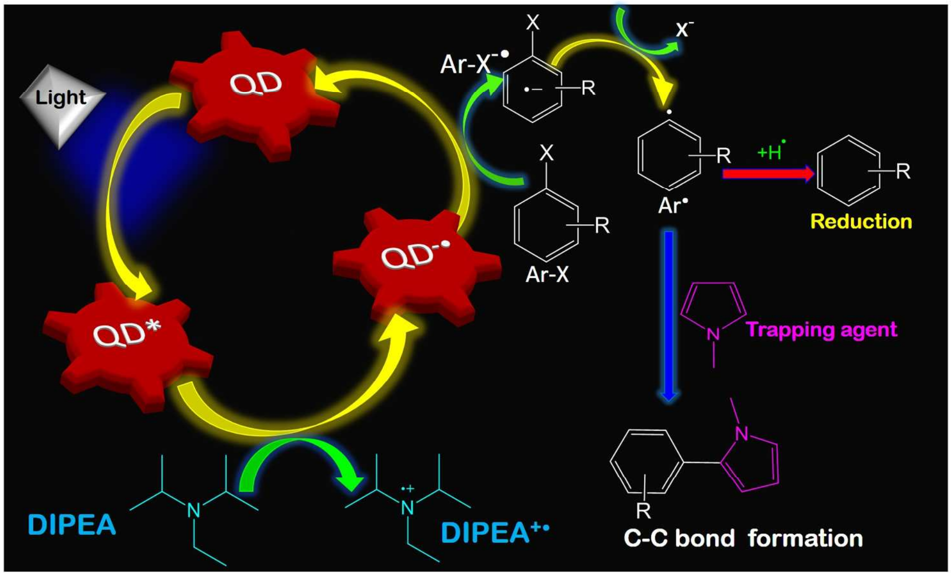

Graphical abstract

340x197mm (150 x 150 DPI)

# Quantum dots in visible light photoredox catalysis: Reductive dehalogenations and C–H arylation reactions using aryl bromides

Anuushka Pal[†], Indrajit Ghosh[‡], Sameer Sapra[†], and Burkhard König[‡]*

[†]Department of Chemistry, Indian Institute of Technology Delhi, Hauz Khas, New Delhi - 110016, India
[‡] Institute of Organic Chemistry, University of Regensburg, D-93040 Regensburg, Germany

*Correspondence to: burkhard.koenig@ur.de

## TABLE OF CONTENTS

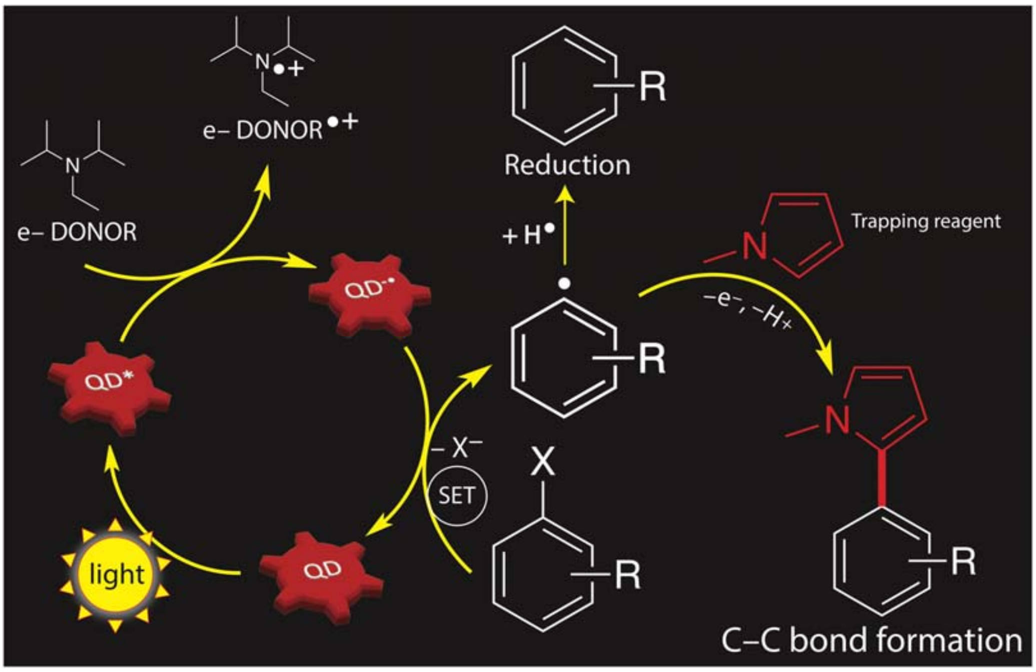

## ABSTRACT

In the recent past, visible light mediated photoredox catalysis has made a huge impact on the development of new synthetic methods under very mild and ecologically benign conditions. Although semiconductor nanocrystals or quantum dots (QDs) posses suitable optoelectronic and redox properties for photoredox catalytic applications, surprisingly, their use for the activation of challenging chemical bonds in the synthesis of organic molecules is little explored. We report here the applications of ZnSe/CdS core/shell QDs for the synthetically important photoredox catalytic activation of carbon–halogen bonds in dehalogenation and C−H arylation reactions using (hetero)aryl halides, as bench stable inexpensive bulk starting materials, under very mild

reaction conditions. The outstanding catalytic activity of ZnSe/CdS core/shell QDs is a direct consequence of the high specific surface area and homogeneity of QDs in solution and their high photostability towards oxidation.

## INTRODUCTION

Semiconductor nanocrystals or quantum dots (QDs) have received enormous attention in the scientific community due to their fascinating optical and electronic properties dependent on size, shape, composition, and heterostructuring.[1–3] Their unique optoelectronic properties render them suitable as promising candidates for applications in different areas, such as photovoltaics,[4–7] light emitting diodes,[8–10] photodetectors,[11,12] biological markers,[13,14] and recently in photo-catalysis.[15,16]

For photocatalysis, QDs are particularly suitable due to their efficient visible light harvesting capabilities, the high extinction coefficients in the visible region, their tunable and size dependent redox potentials. Their solubility can be tuned depending on the ligands exposed at the surface, and the presence of a large fraction of surface atoms provides a highly reactive surface area, leading to more efficient energy or electron transfer processes for catalytic applications.[17] Most importantly, their stability against photoirradiation makes them superior in comparison to conventional organic dyes[18] or commonly used transition metal complexes. Previously, bulk semiconductors and metal nanoparticles have been explored for the photocatalytic degradation of dyes,[19] photo-oxidative degradation and removal of organic pollutants for water purification,[20] water splitting,[21,22] and carbon–carbon bond forming reactions.[16,23,24] However, the heterogeneity imposed by bulk semiconductors retards their catalytic activity. Therefore, considerable efforts have been made in exploring QDs as better photocatalyst compared to their bulk counterparts. Recent reports on nanocrystal-based photocatalysis describe water splitting using cadmium sulfide (CdS) and titanium dioxide,[25–28] ferric oxide,[29] quaternary metal oxides, mixed oxides,[30,31] and the photodegradation of organic molecules such as phenols,[32] benzene, and aromatic ketones by tungsten oxide nanocrystals.[33,34] CdS and cadmium selenide (CdSe) QDs have been used in the photocatalytic reduction of aromatic nitro compounds and azides to amines.[35,36] Niemeyer and Ipe employed QD/enzyme nanohybrids for photocatalyzing the transformation of myristic acid to $\alpha$- and $\beta$-hydroxymyristic acid under UV irradiation.[37] Bernt *et al.* have reported the photochemical carbon disulfide formation from 1,1-dithiooxalate using CdSe QDs under aerobic conditions.[38] Most recently, Li *et al.* have reported the visible light photocatalytic formation of disulfides *via* coupling of a variety of thiols without the need of external oxidants.[39] Jensen *et al.* demonstrated the photocatalytic reduction of nitrobenzene to aniline using CdS QDs.[40] Chauviré *et al.* have investigated the redox behavior of CdSe/ZnS core shell QDs in aqueous medium and monitored the oxidation reaction of 8-oxo-2′-deoxyguanosine, and the reduction of nitrophenylalanine derivatives under visible light.[41]

Although many reports are known on the semiconductor nanocrystal catalyzed photodegradation, surprisingly none on the synthetically important carbon–carbon bond forming reactions using aryl halides.[42,43] Notably, the constructions of carbon–carbon bonds are of particular importance for synthesizing new drugs or fine chemicals, or in simplistic of cases, for the synthesis of arylated arenes or more importantly heteroarenes that are widely used in material science for their interesting electronic and optical properties.

Here, we report our attempts towards the generation of highly reactive aryl or heteroaryl radicals from their corresponding halides for synthetically important arylation reactions using core/shell QDs and visible light. Upon single electron transfer, (hetero)aryl halides (Ar-X, where X= Cl, Br) form their corresponding radical anions, which upon fragmentation and by releasing halide anions generate the corresponding (hetero)aryl radicals. However, photoredox catalytic activation of carbon–halogen bonds in aryl halides *via* single electron transfer in substituted aryl halides possesses, among others, mainly two challenges: (i) their extremely high reduction potentials that are often beyond the reach of many conventional photocatalysts (*e.g.*, $Ru(bpy)_3^{2+}$ or Eosin Y) and (ii) the two step fragmentation kinetics of Ar-X (where X= Cl, Br), which often play a crucial role in determining the feasibility of such photoredox transformations. The generation of aryl radicals from bench stable aryl halides typically involves a strong base, such as potassium tert-butoxide, or nucleophiles under ultraviolet (UV) ($\lambda_{Ex} \leq 350$nm) irradiation (*c.f.*, $S_{RN}1$ reaction mechanism).[44] Murphy and coworkers have shown that the electron transfer to aryl halides could be possible from highly reactive neutral organic reducing agents, such as $N^2$,$N^2$,$N^{12}$,$N^{12}$-tetramethyl-7,8-dihydro-6H-dipyrido[1,4]diazepine-2,12-diamine under UV-A (365 nm) irradiation.[45] Recently, König and co-workers have shown that the reduction of aryl halides is possible using excited doublet states of organic radicals available *via* consecutive photoinduced electron transfer (conPET) processes.[46] We propose core/shell QDs that in the presence of a sacrificial electron donor and upon visible light photoexcitation transfer an electron to the aryl or heteroaryl halides generating aryl or heteroaryl radicals, which are trapped by either hydrogen atom donors or used for C–C bond forming reactions in the presence of suitable reagents.

## RESULTS AND DISCUSSIONS

Our selection of ZnSe/CdS core/shell QDs as the photocatalyst was based on its suitable redox potential for the envisaged conversions (see Figure 1a). We have selected a ZnSe core because of its high reduction potential of –1.8 V *vs* NHE.[31] However, as the excitonic absorption of ZnSe QDs is not in the visible region, we have coated ZnSe with CdS in order to shift the absorption towards the visible blue region and at the same time to form type II junctions for better charge separation.[3,47] Figure 1b displays the steady state absorption and photoluminescence spectra of ZnSe-QDs. The first absorption of ZnSe is observed at 407 nm, and the respective photoluminescence is centered around 420 nm. The sharp photoluminescence spectra with a FWHM of 14 nm indicates the narrow size distribution of the QDs. Figure 1c displays the absorption and the photoluminescence spectra of core/shell ZnSe/CdS QDs. The Stokes shift after the shelling is *ca.* 110 – 120 nm. This high stokes shift indicates the formation of type II junctions in the heterostructures. The powder XRD pattern of the core QDs and core shell QDs match with their bulk counterparts from the JCPDS database (file number 892940) as shown in Figure 1d. The diffraction pattern of core and core/shell QDs reflects the resemblance to the wurtzite crystal of the bulk. In the core/shell structure, the diffraction peaks are shifted to lower 2θ values. The size distribution and size has been calculated by transmission electron microscopy (TEM) and high-resolution transmission electron microscopy (HRTEM) images (Figure 1e and 1f). Here, the average size of core QDs is 3.4 nm and the average size of the core/shell QDs is 4 nm. The TEM images reveal spherical particles that retain their shape after shelling *via* the successive ion layer adsorption reaction (SILAR). The energy dispersive X-ray spectroscopy (EDS) confirms the elemental composition of Zn and Se in ZnSe in an atomic molar ratio of 45 and 55. However, in case of the core/shell QDs the molar composition of Zn, Se, Cd and S are 25, 29, 27 and 17%, respectively. The molar ratio between Cd and Zn indicate the formation of one monolayer.

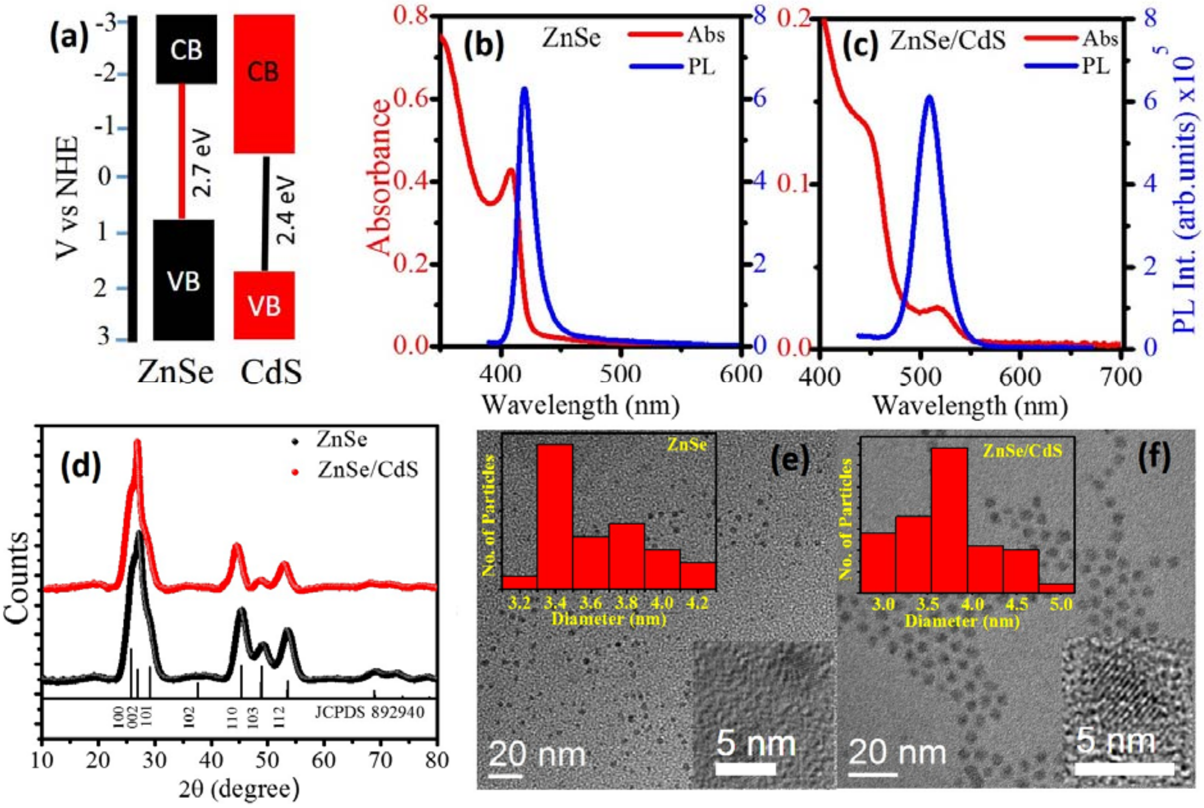

**Figure 1.** (a) Bulk conduction band and valence band positions of ZnSe and CdS. Absorption and photoluminescence spectra of (b) ZnSe, (c) ZnSe/CdS. (d) PXRD pattern of synthesized ZnSe and ZnSe/CdS. TEM images of (e) ZnSe, (f) ZnSe/CdS. The insets of (e) and (f) represent the size distribution histograms and HRTEM images of ZnSe and ZnSe/CdS.

**Applications of QDs in visible light photoredox reduction of aryl halides.** We sought to use these QDs for photoredox reductive generation of aryl radicals from commercially available, inexpensive, and most importantly, bench stable aryl halides. The use of aryl radicals from aryl halides have recently gained enormous interest, because of their importance in C–H arylation reactions with arenes and heteroarenes.[46,48–51]

When a mixture of 2-bromobenzonitrile (model substrate, see Table 1, and Figure 2), core/shell QDs (0.6 mol%), and *N,N*-diisopropylethylamine (DIPEA, as a sacrificial electron donor) was irradiated in hexane with blue LEDs ($\lambda_{Ex}$ = 455 ± 15 nm) benzonitrile was formed as confirmed by GC and GC–MS measurements. To increase the efficiency of this photocatalytic method, the reaction conditions were optimized using various solvents and varying the amount of the electron donor. Among other solvents, hexane and toluene were found to be the best performing solvents for the photoreduction reactions to take place in the presence of 8.0 equiv. of DIPEA. After 24 h, the photoreduction product (*i.e.*, benzonitrile) was obtained in 92% yield. Control experiments confirmed that the presence of QDs, electron donor *i.e.* DIPEA, and blue light photoirradiation are important for the photoredox catalytic reduction reactions to occur.

**Table 1:** Control reactions for reductive dehalogenation of (hetero)aryl halides.

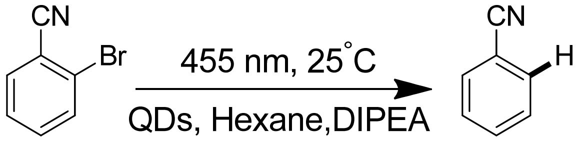

| Entry | Catalyst (mol %) | DIPEA (equiv.) | Reaction Condition | t / h | Yield (%) [a] |
|---|---|---|---|---|---|
| 1 | 0.6 | 8 | 455 nm, $N_2$, 25 °C | 24 | 92 |
| 2 | 0.6 | – | 455 nm, $N_2$, 25 °C | 24 | 8 |
| 3 | – | 8 | 455 nm, $N_2$, 25 °C | 24 | 0 [b] |
| 4 | – | 0 | 455 nm, $N_2$, 25 °C | 24 | 0 [b] |
| 5 | 0.6 | 8 | dark, $N_2$, 25 °C | 24 | 0 [b] |

[a] Determined by GC using naphthalene as an internal standard. [b] The yield is too low to be detected in the GC.

Using the optimized reaction conditions, we explored the scope of the reaction with other aryl halides. This catalytic method is suitable for the reduction of aryl halides possessing electron withdrawing groups (see Figure 2). Electron deficient heteroaromatic compounds can also be dehalogenated in good yields. The photoreduction does not proceed for aryl halides with neutral or electron donating groups that possess higher reduction potentials than the available reduction potential of the QDs, investigated herein, showing the limitation of this method. However, the scope comprises heteroaromatic chlorides, such as pyridines, quinoline, isoquinolines, which were cleanly photoreduced using this catalytic method.

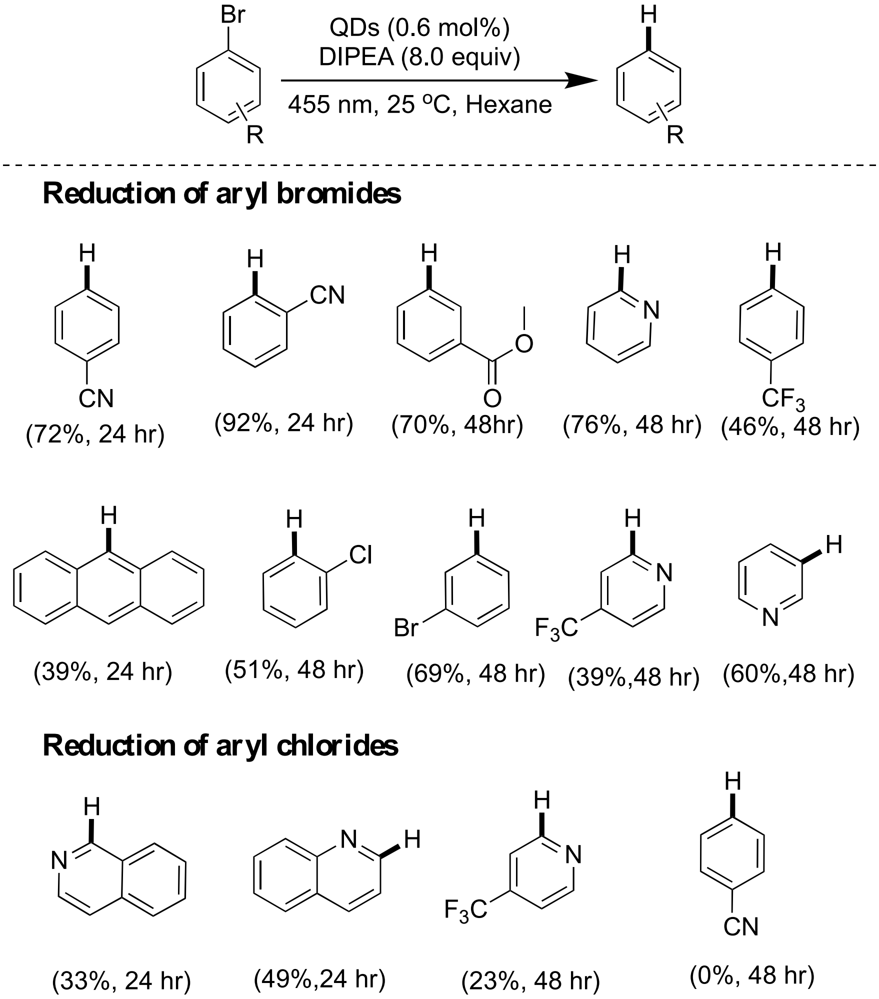

**Figure 2.** Photoreduction of aryl bromides and chlorides. Reaction conditions: Substrate concentration 0.05 mmol; catalyst amount 0.32 $\mu$mol, 0.6 mol%; DIPEA 0.4 mmol, 8.0 equivalents. Photoreduction yields were determined by gas chromatography using naphthalene as an internal standard. Notably, for aryl chlorides unreacted starting materials (when the yields are relatively low) was observed in the GC chromatograms.

Next, we applied the photocatalytic method for C–H arylation reactions using different trapping reagents to capture the generated aryl radicals. The abstraction of hydrogen atoms by aryl radicals from the cation radical of the amine competes with the reductive photoredox catalytic C–H arylation reactions. The amount of added trapping reagent affects the yields of C–C bond formation reactions (more the better). Under this catalytic conditions pyrrole derivatives, including unprotected pyrroles (entry 2 in Figure 3), were found to be effective in trapping the aryl radical in reasonable yields. The yields of the C–H arylation reactions reaches 40% with the remaining amount of the starting material being converted into the corresponding reduction product due to the competing hydrogen abstraction reactions. The mass balance in all photoredox catalytic reactions are very good. Aryl and heteroaryl halide substrates could be used for C–H arylation reactions using cheap pyrrole derivatives as trapping reagents, albeit their use in excess. Alkaloids such as *β*-nicotyrine (entry **3** in Figure 3) could be obtained by simple mixing of commercially available 3-bromopyridine, trapping reagents, QDs in very low catalytic amount, DIPEA, and photoirradiation with visible light under nitrogen.

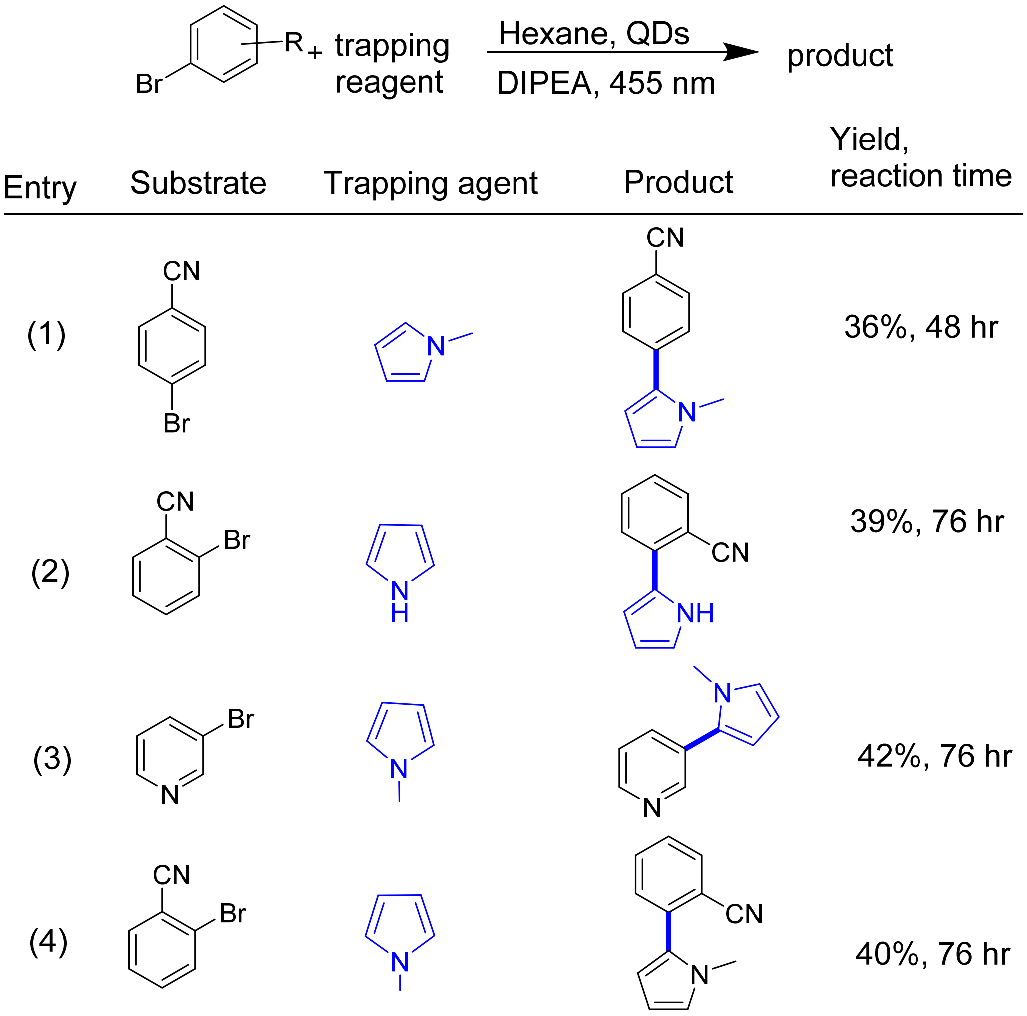

**Figure 3.** C–H arylation of aryl halides using substituted pyrroles as trapping reagents. Reaction conditions: Substrate concentration 0.05 mmol; catalyst amount 0.32 *μ*mol, 0.6 mol%; DIPEA 0.4 mmol, 8 equivalents; pyrroles 1.5 mmol, 30 equivalents. Notably, although not quantified in all cases the reduction products were formed (*via* hydrogen atom abstraction of the aryl radicals from the radical cation of DIPEA) as the byproducts.

**Spectroscopic investigations.** Spectroscopic investigations were performed in order to understand the mechanism of the catalytic cycle. 2-Bromobenzonitrile (model substrate) and DIPEA did not show significant, if any, influence on the absorption spectra of QDs. 2-Bromobenzonitrile also did not have any effect on the photoluminescence spectra of the QDs. However, the photoluminescence spectra of QDs (in this case intensity, PL quenching) changed dramatically upon successive addition of DIPEA (Figure 4). The observed quenching could be attributed to the electron transfer from DIPEA to the excited QDs, as also suggested by previous reports in the literature.[52] However, no ground state spectral shift of QDs in the presence of substrates and DIPEA is observed showing that neither etching nor aggregation of the QDs occurs, indicating their stability.

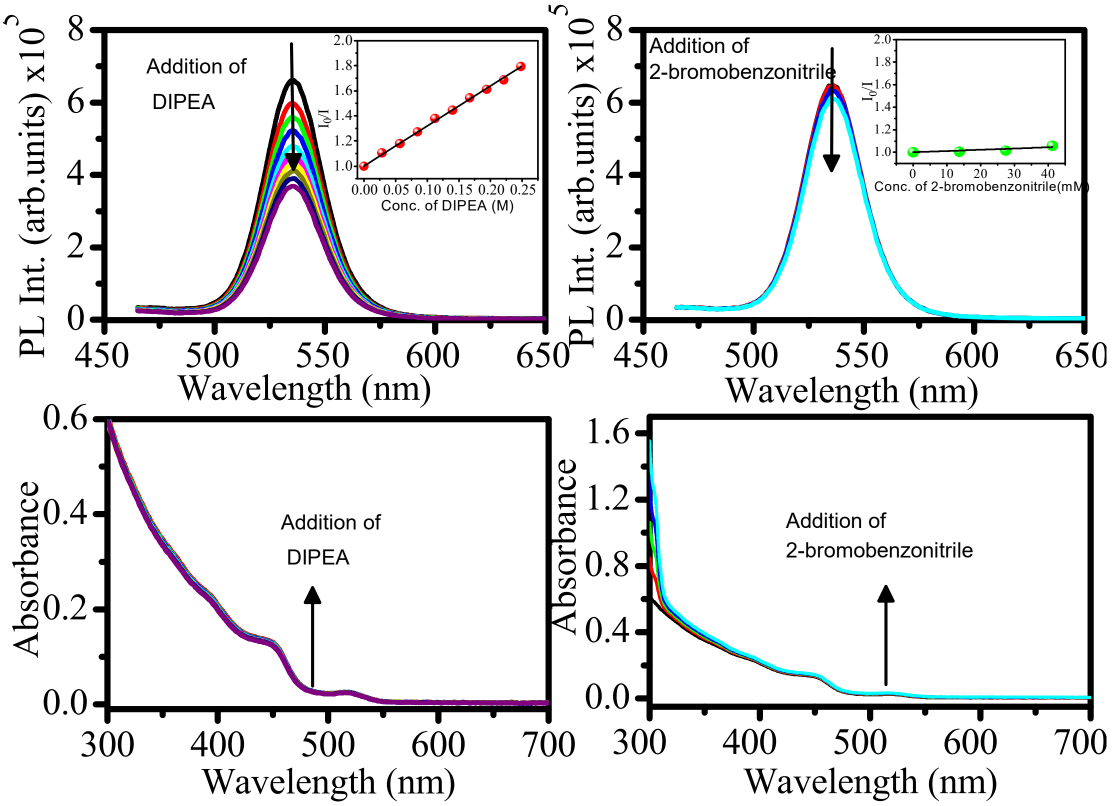

**Figure 4.** Changes in the photoluminescence (in this case intensity) and absorption of QDs upon successive addition of DIPEA ((a) and (c)), and 2-bromobenzonitrile (model substrate, (b) and (d)). In the insets (for Figure a and b) the Stern-Volmer quenching plots are shown. Note that in Figure 3d the increase in the optical density below 300 nm is due to the absorption of 2-bromobenzonitrile.

**Proposed Mechanism of the catalytic cycle.** The spectroscopic investigations, synthetic results along with the literature reports[52] support the proposed photoredox catalytic mechanism depicted in Figure 5. Upon visible light photoexcitation, QDs oxidize DIPEA to form the radical anion of QDs ($QD^{\bullet-}$) and the radical cation of DIPEA ($DIPEA^{\bullet+}$). The QD radical anion transfers an electron to the aryl halide giving the corresponding radical anion $Ar–X^{\bullet-}$.[50,53,54] Upon release of the halide ion ($X^{-}$) an aryl radical is formed, which either abstracts a hydrogen atom, likely from the radical cation of DIPEA, to form the dehalogenated reduction product or is trapped by the investigated pyrrole derivatives, which upon successive oxidation and release of proton yield the C–H arylated products under visible light.[46,48–51]

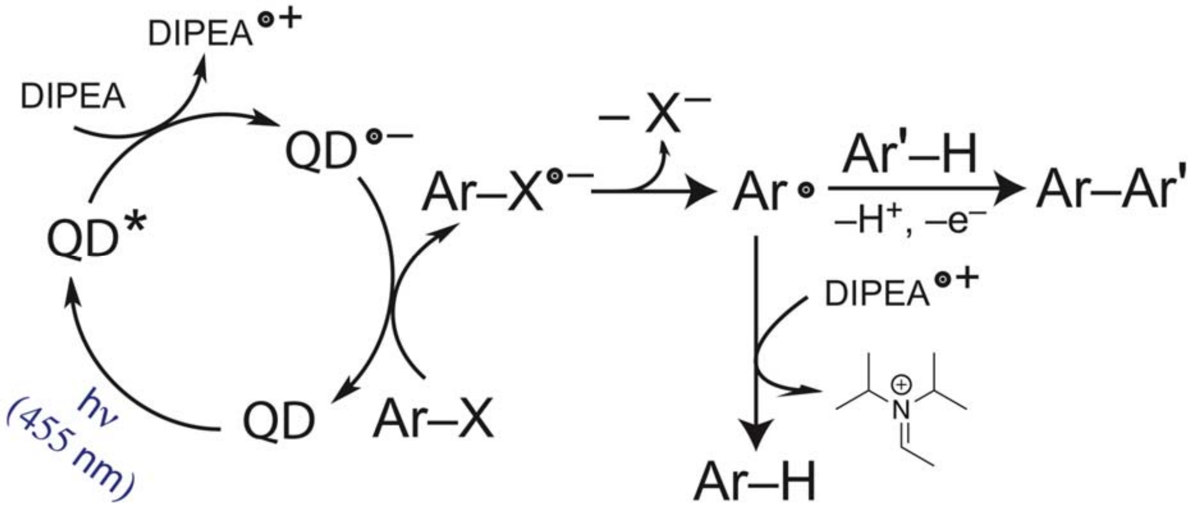

**Figure 5.** Proposed mechanism of the photoredox catalytic cycle.

**Photostability of QDs.** Photoredox catalysts, especially organic dyes and coordination compounds, are readily photodecomposed under visible light photoirradiation requiring high catalyst loadings for photoredox transformations.[49,55] In contrast, the QDs investigated herein are exceptionally photostable when irradiated with blue LEDs ($\lambda_{Ex}$ = 455 ± 15 nm). Indeed, no photodecomposition, indicated by the spectral shift or changes in the optical density, was observed upon prolonged photoirradiation (up to 48 h; see Figure 6). Within the UV–Vis experimental concentration range, most organic dyes decompose within hours. Note that the minimal enhancement that is seen in the absorbance value is due to the evaporation of solvents over the period of time. The photostability of QDs in the presence of DIPEA is slightly reduced as observed from the changes in the absorption spectra as the absorbance of QDs is blue shifted.

The origin of the slightly reduced photostability of QDs in the presence of DIPEA is not clear at present and requires further investigations.

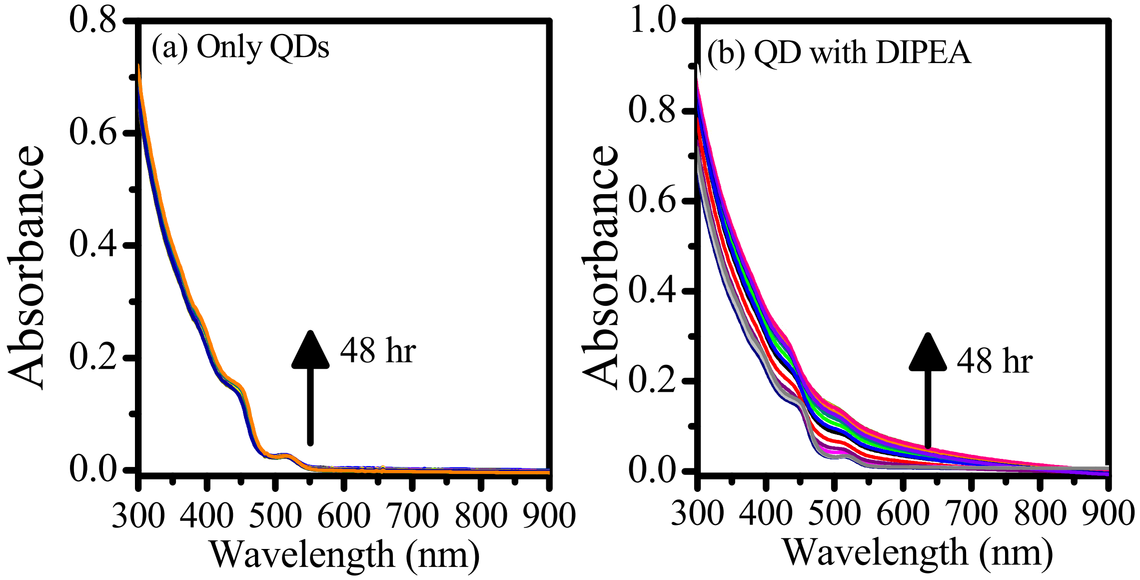

**Figure 6.** The absorbance of QDs on photoirradiation at 455 nm for 48 hours (a) QDs only, (b) QDs with DIPEA. Notably, in Figure 6a the minimal enhancement of the absorbance value is mainly due to the evaporation of solvents over the period of irradiation time. For the changes in the optical density at a particular wavelength with irradiation time, see the supporting information (Figure S2).

## CONCLUSION

QDs have been for the first time employed as visible light photoredox catalyst for the reduction as well as for the synthetically important C–H arylation reactions using aryl halides. The required low catalyst loading, homogeneity in solution, tunable optoelectronic properties, and photostability of the QDs render them as suitable photocatalysts with distinct advantages compared to organic dyes and metal complexes. Upon single electron transfer (hetero)aryl halides (Ar−X) generate the corresponding radical anions (Ar−X•−) that upon fragmentation (and by releasing halide anions) generate the corresponding (hetero)aryl radicals. These radicals either abstract a hydrogen atom from the radical cation of DIPEA to form the reduction products or are trapped by suitable pyrrole derivatives present in the reaction media to afford the C−H arylated products. The catalyst concentration, as low as 0.6 mol%, provides evidence for extremely efficient photoredox catalytic generation of aryl or heteroaryl radicals from (hetero)aryl halides using visible light. The presented results suggest a broader application of QDs in photoredox catalysis that include generation of aryl radicals for the functionalizations of aryl or heteroaryls or formation of carbon–heteroatom bonds, such as carbon–phosphorus bonds (using suitable trapping reagents; for example, trialkyl phosphites) using aryl halides under visible light photoirradiation.

## EXPERIMENTAL SECTION

### Materials Required

Tri-n-octyl phosphine (TOP, 97%), zinc stearate ($Zn(st)_2$, technical grade), selenium powder (99.9%), octadecene (ODE, 90%), sulfur (99.5%), cadmium oxide (CdO,99%), oleic acid (OA), octadecylamine (ODA,90%), 1-butanol were procured from the Sigma Aldrich and were used without further purification, Methanol and hexane (analytical grade) was purchased from VWR and distilled prior to use.

### Synthesis of ZnSe QDs

QDs were synthesized by slight modification of a previously reported hot injection method,[56] in which a mixture of zinc stearate ($Zn(st)_2$, 4 mmol) and 1- octadecene (ODE, 40 ml) was heated at 300 °C in an argon atmosphere until a clear solution was formed. A 4.0 mmol portion of Se was dissolved in 10 mL tri-n-octylphosphine (TOP) in a crimp-capped vial under inert conditions. After attaining 300 °C, the prepared TOPSe solution was injected rapidly into the solution. The growth of NCs was carried out at 290 °C until the desired size of the QDs was achieved as monitored by the UV visible absorption spectrum. After attaining the desired size, the reaction was cooled down to ~ 60 °C and phases were separated by a hexane and methanol mixture (1:1). The solution was centrifuged for 30 minutes giving a solid precipitate and a yellow layer of QDs. Hexane was added to the solid to extract more QDs. The yellow solution containing QDs was purified by precipitating in 1-butanol and re-dispersing in hexane. UV-Vis/photoluminescence spectroscopy and TEM measurements were performed to characterize the resulting nanocrystals for estimation of their size and band gap. Figure 1b shows the absorption and photoluminescence of synthesized quantum dots. The concentration of QDs has been determined by using the method reported by Banin and coworkers (see also the supporting information).[57]

## Core/shell Quantum Dots

### Preparation of injection Stock solutions

A stock solution of 0.4 M cadmium, was obtained by heating of 8 mmol of CdO (1.024g), 32 mmol of oleic acid (10.1 ml) and 9.9 ml of ODE in a 50 ml flask under argon atmosphere at 280 °C under stirring until a clear solution was obtained. The mixture was cooled to 60 °C. A sulfur stock solution of 0.4 M was prepared by heating a 0.4 mmol of sulfur (0.128 g) in ODE (10 ml) to 150 °C under argon.

### Synthesis of core/shell QDs

Core/shell nanocrystals were synthesized by a slightly modified previously reported SILAR method,[47,58] in which the surface of the nanocrystals is cation rich to ensure higher luminescence efficiencies. A $3.8 \times 10^{-6}$ mole of ZnSe core QDs solution, 24 mL of ODE and 9 g of ODA were heated to 100 °C under vacuum for half an hour to remove the traces of solvent. The temperature was raised to 220 °C and the calculated amounts of the stock solutions of sulfur and cadmium were added starting with sulfur. The time between the two successive injections were 10 minutes. After shelling, the reaction mixture was allowed to anneal at 235°C for 20 minutes to improve the crystallinity of the QDs. The QDs solution was allowed to cool to 60 °C and phases were separated by a hexane and methanol mixture and QD were precipitated with acetone. The QDs were re-dispersed in hexane and stored in dark and inert conditions for further use.

## Characterization

All photophysical experiments were performed in hexane at room temperature. UV-Vis absorption spectra were recorded on a Varian Cary 50 spectrophotometer. Fluorescence emission spectra were collected on a Horiba Jobin Yova spectrophotometer with the excitation wavelength of 370 nm for core and 455 nm for core shell QDs. The emission and excitation slit widths were fixed at 2 nm each.

Transmission electron microscope (TEM) images were recorded on a Tecnai $G^2$ 20 electron microscope operated at an accelerating voltage of 200 kV. Samples were prepared on 200-mesh carbon coated Cu grids by dropping very dilute QDs solution dissolved in hexane and allowing the solvent to evaporate. The EDS was collected by Si detector. PXRD was recorded on Agilent Technologies Gemini R Ultra with Cu Kα ($\lambda$= 1.54 Å).

## ACKNOWLEDGEMENTS

We thank the GRK 1626 and DST-SERB Grant No. EMR/2015/000005 for financial support. We are grateful to Prof. Josef Zweck (Physics department, University of Regensburg) for allowing us to carry out the TEM and HRTEM measurements. We thank Prof. Arno Pfitzner (Chemistry department, University of Regensburg) for extending the PXRD facility to us and Dr. Marc Schlosser for carrying out the measurements. AP acknowledges UGC for SRF.

**SUPPORTING INFORMATION.** Materials and methods, general procedures for the photoreduction of arylhalides and C-H arylations, photo of the photochemical set-up, spectroscopic characterization of the C-H arylated products.

## NOTES AND REFERENCES

(1) Brus, L. Electronic Wave Functions in Semiconductor Clusters: Experiment and Theory. *J Phys Chem* **1986**, *90*, 2555–2560.

(2) Brus, L. E. Electron–electron and Electron-Hole Interactions in Small Semiconductor Crystallites: The Size Dependence of the Lowest Excited Electronic State. *J. Chem. Phys.* **1984**, *80*, 4403-4409.

(3) Soni, U.; Pal, A.; Singh, S.; Mittal, M.; Yadav, S.; Elangovan, R.; Sapra, S. Simultaneous Type-I/Type-II Emission from CdSe/CdS/ZnSe Nano-Heterostructures. *ACS Nano* **2014**, *8*, 113–123.

(4) Pal, A.; Saini, P.; Sapra, S. Conjugated-Polymer/Quantum-Confined Nanomaterials-Based Hybrids for Optoelectronic Applications. In *Fundamentals of Conjugated Polymer Blends, Copolymers and Composites*; Saini, P., Ed.; John Wiley & Sons, Inc.: Hoboken, NJ, USA, 2015; pp 163–227.

(5) Sun, B.; Marx, E.; Greenham, N. C. Photovoltaic Devices Using Blends of Branched CdSe Nanoparticles and Conjugated Polymers. *Nano Lett.* **2003**, *3*, 961–963.

(6) Greenham, N.; Peng, X.; Alivisatos, A. Charge Separation and Transport in Conjugated-Polymer/semiconductor-Nanocrystal Composites Studied by Photoluminescence Quenching and Photoconductivity. *Phys. Rev. B* **1996**, *54*, 17628–17637.

(7) Dayal, S.; Kopidakis, N.; Olson, D. C.; Ginley, D. S.; Rumbles, G. Photovoltaic Devices with a Low Band Gap Polymer and CdSe Nanostructures Exceeding 3% Efficiency. *Nano Lett.* **2010**, *10*, 239–242.

(8) Dabbousi, B. O.; Bawendi, M. G.; Onitsuka, O.; Rubner, M. F. Electroluminescence from CdSe Quantum-Dot/polymer Composites. *Appl. Phys. Lett.* **1995**, *66*, 1316-1318.

(9) Gao, M.; Richter, B.; Kirstein, S.; Möhwald, H. Electroluminescence Studies on Self-Assembled Films of PPV and CdSe Nanoparticles. *J. Phys. Chem. B* **1998**, *102*, 4096–4103.

(10) Tessler, N. Efficient Near-Infrared Polymer Nanocrystal Light-Emitting Diodes. *Science* **2002**, *295*, 1506–1508.

(11) Konstantatos, G.; Howard, I.; Fischer, A.; Hoogland, S.; Clifford, J.; Klem, E.; Levina, L.; Sargent, E. H. Ultrasensitive Solution-Cast Quantum Dot Photodetectors. *Nature* **2006**, *442*, 180–183.

(12) Pan, D.; Towe, E.; Kennerly, S. Normal-Incidence Intersubband (In, Ga)As/GaAs Quantum Dot Infrared Photodetectors. *Appl. Phys. Lett.* **1998**, *73*, 1937-1939.

(13) Popović, Z.; Liu, W.; Chauhan, V. P.; Lee, J.; Wong, C.; Greytak, A. B.; Insin, N.; Nocera, D. G.; Fukumura, D.; Jain, R. K.; Bawendi, M. G. A Nanoparticle Size Series for In Vivo Fluorescence Imaging. *Angew. Chem. Int. Ed.* **2010**, *49*, 8649–8652.

(14) Liu, W.; Howarth, M.; Greytak, A. B.; Zheng, Y.; Nocera, D. G.; Ting, A. Y.; Bawendi, M. G. Compact Biocompatible Quantum Dots Functionalized for Cellular Imaging. *J. Am. Chem. Soc.* **2008**, *130*, 1274–1284.

(15) Wilker, M. B.; Schnitzenbaumer, K. J.; Dukovic, G. Recent Progress in Photocatalysis Mediated by Colloidal II-VI Nanocrystals. *Isr. J. Chem.* **2012**, *52*, 1002–1015.

(16) Kisch, H. Semiconductor Photocatalysis-Mechanistic and Synthetic Aspects. *Angew. Chem. Int. Ed.* **2013**, *52*, 812–847.

(17) Pal, A.; Srivastava, S.; Saini, P.; Raina, S.; Ingole, P. P.; Gupta, R.; Sapra, S. Probing the Mechanism of Fluorescence Quenching of QDs by Co(III)-Complexes: Size of QD and Nature of the Complex Both Dictate Energy and Electron Transfer Processes. *J. Phys. Chem. C* **2015**, *119*, 22690–22699.

(18) Resch-Genger, U.; Grabolle, M.; Cavaliere-Jaricot, S.; Nitschke, R.; Nann, T. Quantum Dots versus Organic Dyes as Fluorescent Labels. *Nat. Methods* **2008**, *5*, 763–775.

(19) Li, Y.; Li, X.; Li, J.; Yin, J. Photocatalytic Degradation of Methyl Orange by TiO2-Coated Activated Carbon and Kinetic Study. *Water Res.* **2006**, *40*, 1119–1126.

(20) Pelizzetti, E.; Minero, C. Mechanism of the Photo-Oxidative Degradation of Organic Pollutants over TiO2 Particles. *Electrochim. Acta* **1993**, *38*, 47–55.

(21) Fujishima, A.; Honda, K. Electrochemical Photolysis of Water at a Semiconductor Electrode. *Nature* **1972**, *238*, 37–38.

(22) Zou, Z.; Ye, J.; Sayama, K.; Arakawa, H. Direct Splitting of Water under Visible Light Irradiation with an Oxide Semiconductor Photocatalyst. *Nature* **2001**, *414*, 625–627.

(23) Cherevatskaya, M.; Neumann, M.; Füldner, S.; Harlander, C.; Kümmel, S.; Dankesreiter, S.; Pfitzner, A.; Zeitler, K.; König, B. Visible-Light-Promoted Stereoselective Alkylation by Combining Heterogeneous Photocatalysis with Organocatalysis. *Angew. Chem. Int. Ed.* **2012**, *51*, 4062–4066.

(24) Mitkina, T.; Stanglmair, C.; Setzer, W.; Gruber, M.; Kisch, H.; König, B. Visible Light Mediated Homo- and Heterocoupling of Benzyl Alcohols and Benzyl Amines on Polycrystalline Cadmium Sulfide. *Org Biomol Chem* **2012**, *10*, 3556-3561.

(25) Li, G.-S.; Zhang, D.-Q.; Yu, J. C. A New Visible-Light Photocatalyst: CdS Quantum Dots Embedded Mesoporous $TiO_2$. *Environ. Sci. Technol.* **2009**, *43*, 7079–7085.

(26) Maeda, K.; Domen, K. Photocatalytic Water Splitting: Recent Progress and Future Challenges. *J. Phys. Chem. Lett.* **2010**, *1*, 2655–2661.

(27) Maeda, K. Photocatalytic Water Splitting Using Semiconductor Particles: History and Recent Developments. *J. Photochem. Photobiol. C Photochem. Rev.* **2011**, *12*, 237–268.

(28) Liu, B.; Li, X.-B.; Gao, Y.-J.; Li, Z.-J.; Meng, Q.-Y.; Tung, C.-H.; Wu, L.-Z. A Solution-Processed, Mercaptoacetic Acid-Engineered CdSe Quantum Dot Photocathode for Efficient Hydrogen Production under Visible Light Irradiation. *Energy Env. Sci* **2015**, *8*, 1443–1449.

(29) Kay, A.; Cesar, I.; Grätzel, M. New Benchmark for Water Photooxidation by Nanostructured $\alpha$-$Fe_2O_3$ Films. *J. Am. Chem. Soc.* **2006**, *128*, 15714–15721.

(30) Jafari, T.; Moharreri, E.; Amin, A.; Miao, R.; Song, W.; Suib, S. Photocatalytic Water Splitting—The Untamed Dream: A Review of Recent Advances. *Molecules* **2016**, *21*, 900.

(31) Marschall, R. Semiconductor Composites: Strategies for Enhancing Charge Carrier Separation to Improve Photocatalytic Activity. *Adv. Funct. Mater.* **2014**, *24*, 2421–2440.

(32) Vinu, R.; Madras, G. Kinetics of Simultaneous Photocatalytic Degradation of Phenolic Compounds and Reduction of Metal Ions with Nano-$TiO_2$. *Environ. Sci. Technol.* **2008**, *42*, 913–919.

(33) Tanaka, D.; Oaki, Y.; Imai, H. Enhanced Photocatalytic Activity of Quantum-Confined Tungsten Trioxide Nanoparticles in Mesoporous Silica. *Chem. Commun.* **2010**, *46*, 5286-5288.

(34) Waller, M. R.; Townsend, T. K.; Zhao, J.; Sabio, E. M.; Chamousis, R. L.; Browning, N. D.; Osterloh, F. E. Single-Crystal Tungsten Oxide Nanosheets: Photochemical Water Oxidation in the Quantum Confinement Regime. *Chem Mat* **2012**, *24*, 698–704.

(35) Eskandari, P.; Kazemi, F.; Zand, Z. Photocatalytic Reduction of Aromatic Nitro Compounds Using CdS Nanostructure under Blue LED Irradiation. *J. Photochem. Photobiol. Chem.* **2014**, *274*, 7–12.

(36) Warrier, M.; Lo, M. K. F.; Monbouquette, H.; Garcia-Garibay, M. A. Photocatalytic Reduction of Aromatic Azides to Amines Using CdS and CdSe nanoparticles.*Photochem. Photobiol. Sci.* **2004**, *3*, 859-863.

(37) Ipe, B. I.; Niemeyer, C. M. Nanohybrids Composed of Quantum Dots and Cytochrome P450 as Photocatalysts. *Angew. Chem. Int. Ed.* **2006**, *45*, 504–507.

(38) Bernt, C. M.; Burks, P. T.; DeMartino, A. W.; Pierri, A. E.; Levy, E. S.; Zigler, D. F.; Ford, P. C. Photocatalytic Carbon Disulfide Production via Charge Transfer Quenching of Quantum Dots. *J. Am. Chem. Soc.* **2014**, *136*, 2192–2195.

(39) Li, X.-B.; Li, Z.-J.; Gao, Y.-J.; Meng, Q.-Y.; Yu, S.; Weiss, R. G.; Tung, C.-H.; Wu, L.-Z. Mechanistic Insights into the Interface-Directed Transformation of Thiols into Disulfides and Molecular Hydrogen by Visible-Light Irradiation of Quantum Dots. *Angew. Chem.* **2014**, *126*, 2117–2121.

(40) Jensen, S. C.; Homan, S. B.; Weiss, E. A. Photocatalytic Conversion of Nitrobenzene to Aniline through Sequential Proton-Coupled One-Electron Transfers from a Cadmium Sulfide Quantum Dot. *J. Am. Chem. Soc.* **2016**, *138*, 1591–1600.

(41) Chauviré, T.; Mouesca, J.-M.; Gasparutto, D.; Ravanat, J.-L.; Lebrun, C.; Gromova, M.; Jouneau, P.-H.; Chauvin, J.; Gambarelli, S.; Maurel, V. Redox Photocatalysis with Water-Soluble Core–Shell CdSe-ZnS Quantum Dots. *J. Phys. Chem. C* **2015**, *119*, 17857–17866.

(42) Caputo, J. A.; Frenette, L. C.; Zhao, N.; Sowers, K. L.; Krauss, T. D.; Weix, D. J. General and Efficient C–C Bond Forming Photoredox Catalysis with Semiconductor Quantum Dots. *J. Am. Chem. Soc.* **2017**, *139*, 4250–4253.

(43) Zhang, Z.; Edme, K.; Lian, S.; Weiss, E. A. Enhancing the Rate of Quantum-Dot-Photocatalyzed Carbon–Carbon Coupling by Tuning the Composition of the Dot's Ligand Shell. *J. Am. Chem. Soc.* **2017**, *139*, 4246–4249.

(44) Rossi, R. A.; Pierini, A. B.; Peñéñory, A. B. Nucleophilic Substitution Reactions by Electron Transfer. *Chem. Rev.* **2003**, *103*, 71–168.

(45) Cahard, E.; Schoenebeck, F.; Garnier, J.; Cutulic, S. P. Y.; Zhou, S.; Murphy, J. A. Electron Transfer to Benzenes by Photoactivated Neutral Organic Electron Donor Molecules. *Angew. Chem. Int. Ed.* **2012**, *51*, 3673–3676.

(46) Ghosh, I.; Ghosh, T.; Bardagi, J. I.; Konig, B. Reduction of Aryl Halides by Consecutive Visible Light-Induced Electron Transfer Processes. *Science* **2014**, *346*, 725–728.

(47) Nemchinov, A.; Kirsanova, M.; Hewa-Kasakarage, N. N.; Zamkov, M. Synthesis and Characterization of Type II ZnSe/CdS Core/Shell Nanocrystals. *J. Phys. Chem. C* **2008**, *112*, 9301–9307.

(48) Ghosh, I.; König, B. Chromoselective Photocatalysis: Controlled Bond Activation through Light-Color Regulation of Redox Potentials. *Angew. Chem. Int. Ed.* **2016**, *55*, 7676–7679.

(49) Das, A.; Ghosh, I.; König, B. Synthesis of pyrrolo[1,2-A]quinolines and Ullazines by Visible Light Mediated One- and Twofold Annulation of N-Arylpyrroles with Arylalkynes. *Chem Commun* **2016**, *52*, 8695–8698.

(50) Ghosh, I.; Marzo, L.; Das, A.; Shaikh, R.; König, B. Visible Light Mediated Photoredox Catalytic Arylation Reactions. *Acc. Chem. Res.* **2016**, *49*, 1566–1577.

(51) Marzo, L.; Ghosh, I.; Esteban, F.; König, B. Metal-Free Photocatalyzed Cross Coupling of Bromoheteroarenes with Pyrroles. *ACS Catal.* **2016**, *6*, 6780–6784.

(52) Landes, C.; Burda, C.; Braun, M.; El-Sayed, M. A. Photoluminescence of CdSe Nanoparticles in the Presence of a Hole Acceptor: *n* -Butylamine. *J. Phys. Chem. B* **2001**, *105*, 2981–2986.

(53) Costentin, C.; Robert, M.; Savéant, J.-M. Fragmentation of Aryl Halide π Anion Radicals. Bending of the Cleaving Bond and Activation vs Driving Force Relationships. *J. Am. Chem. Soc.* **2004**, *126*, 16051–16057.

(54) Pause, L.; Robert, M.; Savéant, J.-M. Can Single-Electron Transfer Break an Aromatic Carbon−Heteroatom Bond in One Step? A Novel Example of Transition between Stepwise and Concerted Mechanisms in the Reduction of Aromatic Iodides. *J. Am. Chem. Soc.* **1999**, *121*, 7158–7159.

(55) Graml, A.; Ghosh, I.; König, B. Synthesis of Arylated Nucleobases by Visible Light Photoredox Catalysis. *J. Org. Chem.* **2017**, *82*, 3552–3560.

(56) Reiss, P.; Quemard, G.; Carayon, S.; Bleuse, J.; Chandezon, F.; Pron, A. Luminescent ZnSe Nanocrystals of High Color Purity. *Mater. Chem. Phys.* **2004**, *84*, 10–13.

(57) Dorfs, D.; Salant, A.; Popov, I.; Banin, U. ZnSe Quantum Dots Within CdS Nanorods: A Seeded-Growth Type-II System. *Small* **2008**, *4*, 1319–1323.

(58) Li, J. J.; Wang, Y. A.; Guo, W.; Keay, J. C.; Mishima, T. D.; Johnson, M. B.; Peng, X. Large-Scale Synthesis of Nearly Monodisperse CdSe/CdS Core/Shell Nanocrystals Using Air-Stable Reagents via Successive Ion Layer Adsorption and Reaction. *J. Am. Chem. Soc.* **2003**, *125*, 12567–12575.